The roles of troponin C isoforms in the mechanical function of *Drosophila* indirect flight muscle

Catherine C. Eldred,
Department of Biology & Center for Biotechnology and Interdisciplinary Studies, Rensselaer Polytechnic Institute, Troy, NY 12180, USA

Anja Katzemich,
Department of Biology, University of York, York YO10 5DD, UK

Monica Patel,
Department of Biology & Center for Biotechnology and Interdisciplinary Studies, Rensselaer Polytechnic Institute, Troy, NY 12180, USA

Belinda Bullard, and
Department of Biology, University of York, York YO10 5DD, UK

Douglas M. Swank
Department of Biology & Center for Biotechnology and Interdisciplinary Studies, Rensselaer Polytechnic Institute, Troy, NY 12180, USA

Douglas M. Swank: swankd@rpi.edu

Abstract

Stretch activation (SA) is a fundamental property of all muscle types that increases power output and efficiency, yet its mechanism is unknown. Recently, studies have implicated troponin isoforms as important in the SA mechanism. The highly stretch-activated *Drosophila* IFMs express two isoforms of the Ca^{2+}-binding subunit of troponin (TnC). TnC1 (TnC-F2 in Lethocerus IFM) has two calcium binding sites, while an unusual isoform, TnC4 (TnC-F1 in Lethocerus IFM), has only one binding site. We investigated the roles of these two TnC isoforms in *Drosophila* IFM by targeting RNAi to each isoform. IFMs with TnC4 expression (normally ~90 % of total TnC) replaced by TnC1 did not generate isometric tension, power or display SA. However, TnC4 knockdown resulted in sarcomere ultrastructure disarray, which could explain the lack of mechanical function and thus make interpretation of the influence of TnC4 on SA difficult. Elimination of TnC1 expression (normally ~10 % of total TnC) by RNAi resulted in normal muscle structure. In these IFMs, fiber power generation, isometric tension, stretch-activated force and calcium sensitivity were statistically identical to wild type. When TnC1 RNAi was driven by an IFM specific driver, there was no decrease in flight ability or wing beat frequency, which supports our mechanical findings suggesting that TnC1 is not essential for the mechanical function of *Drosophila* IFM. This finding contrasts with previous work in *Lethocerus* IFM showing TnC1

is essential for maximum isometric force generation. We propose that differences in TnC1 function in *Lethocerus* and *Drosophila* contribute to the ~40-fold difference in IFM isometric tension generated between these species.

Keywords

Locomotion; Asynchronous muscle; Muscle regulation

Introduction

Muscle contraction occurs when a neural discharge triggers the release of calcium ions into the sarcoplasm of a muscle fiber. The calcium ions bind to troponin complexes on the thin filament, producing a shift in the position of tropo-myosin, which partially exposes myosin binding sites on actin. Myosin heads can then bind, further activate the thin filament, and generate force for contraction. When neural stimulation ceases, calcium is re-sequestered into the sarcoplasmic reticulum, Ca^{2+} ions are released from the troponin-complex, and muscle force generation stops as myosin heads are no longer able to bind to actin (Lehman et al. 2009; McKillop and Geeves 1993; Rosenfeld and Taylor 1985; Vibert et al. 1997). The amount of calcium released during activation helps determine the amount of force generated by the muscle by regulating the number of myosin binding sites available on actin. Thus varying calcium level is one way to modulate force levels in muscle.

Once a muscle has been at least partially activated by calcium, force levels in most muscle types can also be modulated by stretch activation (SA) (Pringle 1978). The classic response of an active muscle to a very rapid length increase (stretch) has four phases, an immediate tension increase (phase 1) followed by a quick tension drop (phase 2), a delayed secondary tension increase (phase 3) and a slow tension recovery (phase 4) (Fig. 1). Phase 3 of the tension transient is SA, the delayed rise in force following rapid muscle lengthening. The opposite and complimentary phenomenon to SA is shortening deactivation (SD), a delayed drop in force following shortening (Josephson et al. 2000). SA and SD increase work and power generation in muscle types that cyclically lengthen and shorten because the delayed force changes result in increased force generation during shortening and decreased force during lengthening, compared to muscle types with less SA and SD. SA and SD improve muscle efficiency by reducing the energy needed to release calcium into the muscle and to actively pump it out during each contraction cycle. This occurs to a small degree in some skeletal muscle types that have a small amount of SA and SD and are used cyclically (Pringle 1981; Syme and Josephson 1995). Cardiac muscle displays a moderate amount of SA, which helps increase contractility in response to venous return (filling), as stretch of heart muscle during diastole results in greater subsequent force generation during systole (Moss and Fitzsimons 2002; Syme and Josephson 1995). SD increases filling during diastole by helping increase the rate and extent of ventricular relaxation. The highest level of SA occurs in insect indirect flight muscle (IFM). In IFM, calcium release is only required to prime the muscle for contraction. Calcium cycling per contraction cycle is not required. SA and SD modulate force levels during each contraction cycle, enabling work and power generation at a relatively constant calcium concentration (Josephson et al. 2001).

While the mechanism by which calcium varies force is fairly well understood, the mechanism behind SA is not known. Suggested mechanisms include the thick and thin filament lattice-matching model (Wray 1979), stretching of connecting filaments running between the Z-disc and the ends of the thick filaments which decreases filament lattice spacing (Fukuda and Granzier 2005; Granzier and Wang 1993), strain-induced alterations in myosin kinetics (Thorson and White 1983), phosphorylation of the myosin regulatory light chain increasing cross-bridge recruitment (Dickinson et al. 1997; Tohtong et al. 1995) and myosin-troponin bridges relieving tropomyosin's blocking of actin binding sites (Bullard and Pastore 2011; Perz-Edwards et al. 2011).

Recent studies indicate that variations in troponin C (TnC) isoforms may be linked to the SA mechanism. TnC is one of the subunits that along with troponin-I (TnI, the inhibitory subunit) and troponin-T (TnT, the tropomyosin-binding subunit), make up the troponin complex. Each troponin complex binds to a tropomyosin molecule to form repeating regulatory units along the thin filament. TnC is an 18 kDa, calcium-binding protein with four EF-hand motifs, allowing the possibility of binding up to four Ca^{2+} ions. In vertebrates, the C-terminal domain contains two high-affinity sites, which bind Ca^{2+} and Mg^{2+} and are responsible for the integration of TnC into the troponin complex. The N-terminal domain of skeletal TnC contains lower–affinity, regulatory Ca^{2+}-binding sites. Calcium binding to these sites releases TnI from an inhibitory position on actin, which is followed by movement of tropomyosin to expose myosin-binding sites and the development of force (Gagne et al. 1998; Lehman et al. 2009; McKillop and Geeves 1993). Vertebrate cardiac TnC has only one N-terminal regulatory site, which binds calcium at physiological concentrations. The highly stretch-activated IFM contains two TnC isoforms, TnC4 and TnC1, which are encoded by separate genes. TnC4 is unusual in that it binds a single Ca^{2+} ion in the C-terminal domain with high affinity. TnC1, like the TnC of most invertebrate muscles (Collins 1991), binds two calcium ions, one in the N-domain, which is regulatory, and one with higher affinity in the C-domain (Agianian et al. 2004). Previous mechanical measurements with *Lethocerus* IFM fibers in which TnC isoforms were exchanged within the troponin complex suggest that TnC4 (TnC-F1 in *Lethocerus* IFM) is required for SA, while TnC1 (TnC-F2 in *Lethocerus* IFM) is required for calcium -activated isometric tension (Agianian et al. 2004; Krzic et al. 2010).

To investigate the intriguing *Lethocerus* TnC findings, we turned to the *Drosophila* system to make use of its large array of genetic tools for manipulating muscle proteins and its mechanically testable IFM (Swank 2012). Using *Drosophila* also enabled us to determine if the findings in *Lethocerus* apply to other insects that also possess highly stretch-activated IFM. Not all insect flight muscles are stretch-activated, and SA has evolved independently in different orders (Cullen 1974). Thus, the mechanisms of SA and the roles of TnC isoforms might vary between distant insect species. We used RNAi to independently decrease expression of each TnC isoform in *Drosophila* IFM. TnC4 knockdown resulted in complete loss of flight ability, IFM SA, muscle power generation, active isometric tension, and sarcomeric integrity. The structure of the IFM in TnC1-knockdown flies was similar to that of wild type. No differences in isometric tension, SA force, power, calcium sensitivity, or flight ability compared to the control line were observed. We conclude that unlike

Lethocerus IFM where TnC1 plays a major role in isometric tension generation, in *Drosophila* IFM, which produces much lower isometric tension, TnC1 is not essential for basic muscle mechanical functions.

Materials and methods

Genetic crosses

For RNAi experiments, UAS-responder lines of TnC4 (transformant ID 51741) and TnC1 (transformant ID 104894) were obtained from the Vienna *Drosophila* RNAi Center (http://www.stockcenter.vdrc.at). These were crossed to the general muscle driver line *Mef2-GAL4* or to the IFM-specific *UH3-GAL4* line (from U. Nongthomba, IISc, Bangalore). Males of the *UAS-RNAi* lines were crossed with virgin females of the driver lines. Crosses were performed at 25 °C. Flies were selected at 2–3 days post-eclosure, when IFMs are fully formed.

Confocal microscopy

Half thoraces of wild type flies and flies from the RNAi lines were glycerinated in 0.1 M NaCl, 20 mM Na-phosphate pH 7.2, 5 mM $MgCl_2$, 5 mM EGTA, 5 mM DTT, 0.5 % Triton X-100, 50 % glycerol overnight at -20 °C. IFMs were dissected from glycerinated half thoraces, washed in relaxing solution (0.1 M NaCl, 20 mM Na-phosphate pH 7.2, 5 mM $MgCl_2$, 5 mM ATP, 5 mM EGTA) with protease inhibitors, and separated into myo-fibrils (Burkart et al. 2007). Myofibrils were labeled with primary antibody for 1 h, washed in relaxing solution, then labeled with secondary antibody and rhodamine-phalloidin (Sigma) for 1 h (Burkart et al. 2007; Katzemich et al. 2012). Primary antibodies, rabbit anti-obscurin (Ig14-16) (Burkart et al. 2007) and monoclonal rat anti-kettin MAC 155 (Lakey et al. 1993) were diluted 1:100 in relaxing solution. Secondary antibodies were FITC anti-rabbit and Cy-5 anti-rat (Jackson ImmunoResearch, USA). Myofibrils mounted in ProLong-Gold antifade solution (Invitrogen) were examined with a Zeiss LSM510 confocal microscope with 63 × oil-immersion objective and images were processed with LSM software.

Electron microscopy

Half thoraces were incubated in 1 % Triton X-100 in relaxing solution (150 mM KCl, 5 mM MOPS pH 6.8, 5 mM $MgCl_2$, 5 mM EGTA, 5 mM ATP, 5 mM NaN_3) with protease inhibitors for 2 h at 4 °C, then incubated overnight in the same buffer with 50 % glycerol instead of Triton X-100 (Farman et al. 2009; Reedy and Beall 1993; Reedy et al. 1989). Thoraces were incubated a second time in Triton X-100 in relaxing solution, followed by incubation with 50 % glycerol in relaxing solution; both incubations were for 2 h. Thoraces were then washed in rigor solution (40 mM KCl, 5 mM MOPS, pH 6.8, 5 mM EGTA, 5 mM $MgCl_2$, 5 mM NaN_3) and fixed in 3 % glutaraldehyde, 0.2 % tannic acid in 20 mM MOPS pH 6.8, 5 mM EGTA, 5 mM $MgCl_2$, 5 mM NaN_3 for 2 h at 25 °C. This was followed by washing, first in rigor solution, then in 100 mM Na-phosphate pH 6.0, 10 mM $MgCl_2$. Samples were fixed in 1 % osmium tetroxide, block stained in 2 % uranyl acetate, dehydrated in ethanol and embedded in Epon. Sections were stained with 7 % uranyl acetate for 30 min, followed by Sato lead stain for 1 min. Sections were examined with a FEI Tecnai Biotwin electron microscope at 120 kV.

SDS-PAGE and immunoblotting

Samples were analyzed using 10 cm long 15 % SDS-PAGE gels. Long gels are needed to resolve TnC4 and TnC1 (Qiu et al. 2003). IFMs were dissected from glycerinated half thoraces and dissolved in sample buffer with 6 M urea and protease inhibitors. Gels were immunoblotted and incubated in rat monoclonal antibodies to TnC (MAC 352), which reacts with both TnC4 and TnC1 and TmH (MAC 81), both diluted 1:5,000 (Agianian et al. 2004), followed by goat anti-rat secondary antibody (Jackson ImmunoResearch, USA). Blots were developed using chemiluminescent substrate (Millipore). The relative amounts of TnC4 and TnC1 in IFMs were estimated by scanning blots of IFMs from wild type flies and flies from RNAi lines; the area of peaks was measured using NIH ImageJ.

Muscle mechanics

Dissection and mechanics experiments on skinned fibers from 2 to 3 day old female *Drosophila* were performed as described previously (Swank 2012). Briefly, skinned single fibers were attached to the muscle mechanics apparatus using aluminum T-clips, and activated at pCa 5.0. Optimal fiber length was determined by lengthening the fiber until maximum power generation occurred as measured using sinusoidal analysis (see below). Isometric tension, step analysis, work loops or additional sinusoidal analysis protocols were subsequently performed at this optimal length at 15 °C.

Isometric tension and stretch-activation analysis

Isometric tension was measured at pCa 8.0 and 5.0. A rapid lengthening step 1 % muscle length (ML) over 0.5 ms was performed to measure stretch-activated tension (F_{SA}) at pCa 8.0 (relaxed) and pCa 5.0 (active). The assay and analysis were performed as described previously (Wang et al. 2011). Briefly, the pCa 5.0 tension value at the peak of phase 3 was measured. The isometric tension value immediately prior to the lengthening step was subtracted to determine the amount of stretch-activated tension (A_{SA}). Passive stretch tension (P_{SA}) was obtained the same way as A_{SA} except the lengthening step was performed at pCa 8.0, and since there is no phase 3 in passive fibers, we used the time point that the peak of phase 3 occurred after the lengthening step in active fibers to determine the time point to make the passive stretch tension measurement. To obtain net SA tension (F_{SA}), P_{SA} was subtracted from A_{SA}.

Work loop power measurements

To measure maximum power generation while the muscle was undergoing longer ML changes than we used for sinusoidal analysis, we used work loop analysis. During work loop analysis the muscle fiber length was oscillated through a sinusoid waveform of ten cycles at 100 Hz or 125 Hz and amplitudes of 0.75 or 1 % ML. The resulting tension and muscle length traces were recorded and analyzed to calculate work per cycle and power as described previously (Wang et al. 2011). After each work loop run, sinusoidal analysis was performed to monitor the fibers for possible decreases in performance due to run down.

Sinusoidal analysis

We used small amplitude sinusoidal analysis to determine the optimal length during initial set up and to determine power generation characteristics over a wider range of calcium concentrations and ML oscillation frequencies than is possible with the work loop technique. Power and the frequency at which maximum power was generated (f_{max}) were calculated. The assay was performed and analyzed as previously described (Wang et al. 2011).

Flight assays

Three day old flies were flight tested at 25 °C (Wang et al. 2011). Flies were released inside a perspex box illuminated from above, and scored for the ability to fly up, horizontally or down. The wing beat frequency of a fly was determined using an optical tachometer as previously described (Hyatt and Maughan 1994).

Results

Expression levels of TnC isoforms in the IFM

Expression of the two isoforms of TnC in IFM was reduced by targeted RNAi. RNAi combined with the *GAL4-UAS* system can be used to reduce expression in specific muscles or in all muscles. The driver line *UH3-GAL4* targets only the IFM while *Mef2-GAL4* targets all *Drosophila* muscles. The driver lines were crossed with *UAS-tnc1-IR* and *UAS-tnc4-IR* lines to knock down TnC1 and TnC4, respectively. Two different *UAS-tnc1-IR* and *UAS-tnc4-IR* lines were used. The effect on the IFM was the same for the two lines, showing that off-target effects were unlikely.

The expression of TnC in IFM was assessed in western blots of wild type and TnC-knockdown flies (Fig. 2). TnC1 and TnC4 could be resolved on long gels. In wild type IFM, the ratio of TnC4:TnC1 was about 10:1. No TnC4 was detected in the IFM of *UH3-GAL4;UAS-tnc4-IR* or *Mef2-GAL4;UAS-tnc4-IR* flies. However, expression of TnC1 in these flies was greatly increased: with the *UH3-GAL4* driver, TnC1 was up regulated to 160 % of the total TnC in wild type flies, and with *Mef2-GAL4*, TnC1 expression was increased to the same level as the total TnC in the wild type. No TnC1 was detected in *UAS-tnc1-IR* flies driven by *UH3-GAL4* or *Mef2-GAL4*, while the expression of TnC4 in these flies was similar to that of the wild type. Therefore, the lack of TnC4 is compensated by an increase in the expression of TnC1, but lack of TnC1 does not appreciably affect expression of TnC4 (Fig. 2).

Structure of IFM myofibrils in TnC knockdown flies

The overall structure of myofibrils was determined by labeling actin and the M-Line and Z-disc (Fig. 3). In both TnC1 and TnC4 RNAi lines, H-zones were visible and sarcomere lengths were similar to that of the wild type. Reduced expression of TnC1 in the IFM of *UAS-tnc1-IR* flies with *UH3-GAL4* or *Mef2 GAL4* drivers had no effect on the regularity of the M-lines and Z-discs. In contrast, reduced expression of TnC4 in *UAS-tnc4-IR* flies with both drivers resulted in dot-like M-lines and Z-discs that were more diffuse than in the wild type. The effect of down-regulating TnC4 on the filament lattice in IFM is seen in electron micrographs (Fig. 4). The Z-disc and M-line were disrupted in *UAS-tnc4-IR* flies with the

UH3-GAL4 or the *Mef2-GAL4* driver. Thick and thin filaments were poorly aligned, with some irregular gaps between them. The effect on the IFM structure was more extreme with the *Mef2-GAL4* driver: Z-discs were frequently discontinuous and the periphery of the myofibril was frayed. Sarcomere lengths in TnC4 knockdown IFMs with both drivers were similar to those of the wild type; this is seen in an overview of myofibrils (Fig. 5). Thus, TnC4 is required for normal IFM ultrastructure even when the amount of TnC1 is up regulated to be equal to, or greater than, the total TnC in wild type IFM.

Calcium-activated tension

To test if TnC1 is important for calcium-activated isometric tension, we measured isometric properties of *Mef2-Gal4;UAS-tnc1-IR* fibers. We found that active, passive, and net tensions of TnC1-knockdown fibers were not significantly different from wild type (Table 1). *Mef2-Gal4*-driven TnC4-knockdown fibers produced 48 % of wild type fiber passive isometric tension at pCa 8.0 (Table 1). However, there was no increase in tension with calcium addition, as the tension value at pCa 5.0 was not significantly different from that at pCa 8.0 (Table 1).

Stretch-activated tension

Our skinned, wild-type *Drosophila* indirect flight muscles displayed the typical stretch-activation response to a very rapid increase in length. The response consisted of an immediate tension increase (phase 1), a quick tension drop (phase 2), a delayed secondary tension increase (phase 3) and a slow tension recovery (phase 4) (Fig. 6). Phase 3 of the tension transient is SA. Knocking down TnC1 did not alter IFM stretch-activation properties: the values of total, passive and net stretch-activated tension were not significantly different from wild type (Table 2).

While phase 1 and phase 2 were still apparent, TnC4-knockdown IFMs did not produce the characteristic phase 3 force (F_{SA}) increase at any of the pCa values assayed (Fig. 6b). This suggests TnC4 is required for SA. However, we have previously observed that poor muscle ultrastructure decreases muscle mechanical performance (Swank et al. 2002, 2004). Thus, since the normally highly ordered IFM fiber lattice is disrupted by the TnC4 knockdown, this disruption could be responsible for no detectable phase 3 rather than lack of TnC4 protein.

Power generation, work loop analysis

Wild type and TnC1-knockdown IFM work and power generation were not significantly different when measured under identical work loop conditions (Fig. 7a; Table 3). The ML change and frequency conditions chosen were previously shown to be optimal for wild type IFM power production (Wang et al. 2011). Varying these conditions also showed no significant differences between wild type and TnC1-knockdown fibers (Fig. 7b).

In contrast, TnC4-knockdown fibers were incapable of producing net positive work and power under any frequency, length change or calcium concentration tested. The clockwise work loops of TnC4 fibers indicate work absorption (negative work) by the fibers (Fig. 7a, b; Table 3).

Power generation, sinusoidal analysis

To test the ability of IFM fibers to generate oscillatory power at different pCas, we performed small amplitude sinusoidal analysis (0.125 % ML). This also tests a broader frequency range (0.5–500 Hz) than we could examine with the larger amplitude work loops and allowed us to test more calcium concentrations because the small length changes cause minimal fiber run-down while successive larger amplitude loops slowly decrease fiber performance (Swank 2012; Wang et al. 2011).

TnC1-knockdown fibers generated the same amount of power as control fibers at all ML change frequencies tested, including f_{max}, the frequency at which maximum power was generated (Fig. 7c; Table 4). This supports our observations using work loop analysis. Maximum power at all pCas tested was not significantly different (Fig. 7d). When fitted with the Hill equation, the pCa_{50} and Hill coefficient of TnC1-knockdown fibers was not significantly different from control fibers (Fig. 7d; Table 4). The frequency at which maximum power was generated was not different between TnC1-knockdown fibers and control fibers at any pCa tested (Fig. 7e). TnC4-knockdown IFM fibers showed minimal or no power generation at all frequencies and pCas tested (Fig. 7c). The short amplitude length change during sinusoidal analysis (0.125 % ML) enabled some fibers to produce very small amounts of positive power. In contrast, the much larger amplitudes (0.75 %) during work loop assays greatly increased negative work during muscle lengthening causing high net negative work and power (Table 3).

Flight assays

The effect of TnC1 knockdown on flight ability was dependent on which driver was used. The flight ability of *UAS-tnc1-IR* flies was not significantly different from that of wild type flies when RNAi expression was driven by the *UH3-Gal4* driver (Fig. 8). Flight indexes and wing beat frequencies (Table 5) were not significantly different from the control line. When the *UAS-tnc1-IR* line was driven by *Mef2-GAL4,* we observed a slight decrease in flight ability. Over 60 % flew upwards with about 15 % flying horizontally and the rest flightless (Fig. 8). Wing beat frequency at 15 °C decreased 6 % (Table 5). *UAS-tnc4-IR* flies driven by either *UH3-GAL4* or *Mef2-GAL4* were flightless.

Discussion

SA of IFM may occur through a reversible change in the thin filament that results in recruitment of additional crossbridges at a constant priming concentration of calcium (Agianian et al. 2004; Bullard and Pastore 2011; Iwamoto et al. 2010; Linari et al. 2004; Perz-Edwards et al. 2011). Experiments with isolated fibers of *Lethocerus* IFM have shown that thin-filament regulation is affected by the two isoforms of TnC in the troponin complex: TnC-F1 is needed for stretch activated force and TnC-F2 for maximum isometric force. *Drosophila* IFM has equivalent TnC iso-forms (TnC4 and TnC1), which are present in the same proportion as in *Lethocerus* IFM. We have used RNAi techniques to down-regulate the two isoforms in *Drosophila* IFM; the aim was to find the effect of each isoform independently on the highly stretch activated IFM.

Mechanical properties of IFM

We studied the mechanical properties of IFMs from the TnC4-knockdown line driven by *Mef2-GAL4* because this driver caused up-regulation of TnC1 to an amount equal to the total TnC in wild type IFM. This line produced nonfunctional IFMs. We observed no power generation, SA (phase 3), or significant amounts of active isometric tension. If we had seen some evidence of SA or power generation from any of the TnC4-knockdown IFM fibers, this would have suggested TnC4 was not essential for SA, but we did not.

Our investigation into the role of TnC1 produced the unexpected finding that TnC1 does not appear to be required for *Drosophila* IFM function. We could not find any mechanical differences between TnC1-knockdown fibers and control fibers. We did not see any change in the force response after a rapid lengthening step or in power generation characteristics, which we independently evaluated using both the work loop technique and sinusoidal analysis. We also investigated calcium sensitivity because TnC is a critical component in determining a muscle fiber's response to calcium, and because the two IFM isoforms have different calcium binding properties. However, we found no change in pCa_{50} or Hill coefficient when we varied calcium concentration and measured power generation.

How confident are we that TnC1 is not important for *Drosophila* IFM mechanical function? Perhaps the influ-ence of TnC1 is very small since it is only ~10 % of total TnC in *Drosophila* IFM. If the influence on mechanical properties is proportional to the amount of TnC, a 10 % change in some of the mechanical properties might not be detectable by some of our measurements. For example, we likely cannot detect a 10 % difference in active isometric tension because tension measurements from *Drosophila* IFM have a high degree of error relative to other muscle preparations. This is simply because active isometric tension level is very low and the signal to noise ratio is poor. Sinusoidal analysis is our most sensitive technique, which is why we used it to look at calcium sensitivity. However, sinusoidal analysis did not detect any changes in calcium sensitivity. *Lethocerus* IFM TnC-F2 (TnC1) expression is also just 10 % of total TnC (Krzic et al. 2010), but the mechanical impact of its removal from IFM fibers was very obvious. Isometric tension was reduced by about ~50 % and work production increased two to threefold at pCa 4.75 in chemically extracted fibers with 100 % TnC-F1 compared to wild type (Krzic et al. 2010), The magnitude of these differences should easily have been detected by our *Drosophila* mechanics experiments if TnC1 played as important a mechanical role in *Drosophila* as it does in *Lethocerus* IFM.

Another possibility is that TnC1 influences a mechanical property we did not measure. For example, using our skinned fiber preparation, we cannot measure calcium-driven activation and relaxation rates because of the necessity of using successive solution exchanges to change calcium concentrations (Swank 2012). Alternatively, perhaps TnC1 is not involved in *Drosophila* IFM mechanical function at all and is instead important for some other aspect of calcium buffering that is needed in a live fiber.

The interpretation that TnC1 is not important for *Drosophila* IFM mechanical function was supported by the flight assay results of the TnC1-knockdown line driven by *UH3-GAL4*. We did not observe any decrease in flight performance of this line compared to wild type. The

slightly different flight results for the two TnC1-knockdown lines were initially confusing, but can most likely be explained by the specificity of the drivers. *UH3-GAL4* only drives RNAi expression in the IFM, whereas *Mef2-GAL4* drives expression in all *Drosophila* muscles. Thus, the *Mef2-GAL4* driver likely also decreases TnC1 expression in the jump muscle and other tubular muscles of the thorax where TnC1 transcripts have been detected (Herranz et al. 2004). This could explain why this line was slightly flight impaired while the line driven by *UH3-GAL4* was not. The direct flight muscles are known to modulate wing beat frequency and hence flight ability (Lehmann and Dickinson 1997; Tu and Dickinson 1996), and the jump muscle powers the take-off that initiates flight (Card and Dickinson 2008; Zumstein et al. 2004).

While we did not observe any differences in flight index or WBF for the IFM specific TnC1-knockdown flies, there are other aspects of flight we could not measure due to a lack of equipment, such as high speed video cameras, that would have enabled more sophisticated measurements. Perhaps TnC1 enables a faster take-off by producing isometric tension in response to calcium influx, before TnC4 responds to stretch. Activation of the IFM by stretch requires the muscle to be under tension. The higher affinity of TnC1 for TnI, compared to TnC4—attributed to the two TnI binding sites—(Krzic et al. 2010), may have the effect of activating the thin filament more rapidly than is the case with TnC4 alone. Conversely, TnC1 may be needed for quickly ending IFM oscillations when a fly lands.

The *Drosophila* IFM TnC1-knockdown results contrast with previous work on *Lethocerus* IFMs. TnC-F2 (TnC1) is needed for the production of maximum isometric tension in *Lethocerus* IFM (Agianian et al. 2004; Krzic et al. 2010). We propose that the different results are due to differences in the mechanical characteristics of the IFMs between the two species and how their IFMs are used. *Lethocerus* and *Drosophil*a both need to generate high amounts of power for flight. However, they go about this in very different manners. *Lethocerus* IFMs generates high forces at relatively low muscle speeds while *Drosophila* takes the high speed, low force approach. From mechanical measurements on isolated fibers, we know that *Lethocerus* IFMs generate about 40-fold higher isometric tension than *Drosophila* IFMs, ~120 and ~3 mN/ mm^2, respectively (Agianian et al. 2004; Yang et al. 2008). The frequency at which *Drosophila* IFM maximum power is generated is ~150 Hz at 15 °C, compared to ~2–4 Hz for isolated *Lethocerus* fibers at 23 °C (Agianian et al. 2004; Linari et al. 2004; Ramanath et al. 2011; Wang et al. 2014). Other very rapidly oscillating muscle types have also been found to generate very low forces. For example, the toadfish swim bladder muscle, which operates at 200 Hz at 25 °C, generates 10 % of the isometric tension produced by the toadfish's skeletal muscle fiber types (Rome et al. 1999). In addition to differences when powering flight, *Lethocerus* IFMs are used for a function that *Drosophila* IFMs do not perform. *Lethoce-rus* IFMs perform rapid isometric contractions during a warm-up period prior to take-off (Esch et al. 1991; Heinrich 1996). These contractions are likely activated by TnC-F2 (corresponding to TnC1 in *Drosophila*). Thus, perhaps *Lethocerus* TnC-F2 (TnC1) evolved to help generate relatively high tension levels, but evolutionary pressures in *Drosophila* favored a TnC1 that does not cause increased isometric tension.

Our finding that TnC1 does not contribute to isometric tension could also explain the difference in optimal calcium concentrations for SA and power production of *Lethocerus* IFMs compared to *Drosophila* IFMs. This reasoning is predicated on the proposal that IFM SA can only occur on a partially calcium activated thin filament (Bullard and Pastore 2011; Perz-Edwards et al. 2011). *Lethocerus* produces maximum SA tension at calcium concentrations ~pCa 6.1, that produce sub-maximum calcium activated isometric tension levels (Agianian et al. 2004; Krzic et al. 2010; Linari et al. 2004). Because *Lethocerus* TnC1 causes increased calcium-activated isometric tension, *Lethocerus* IFMs have to operate at subsaturating levels of calcium for SA and SD to occur. This was shown by the finding that *Lethocerus* IFM can produce maximal work and power at higher than normal calcium concentrations in fibers that have TnC-F1, but no TnC-F2 (Krzic et al. 2010). In contrast, *Drosophila* SA tension and power is highest at the same calcium concentration that produces maximum isometric tension, ~pCa 5.0 (Wang et al. 2011). Perhaps without TnC1 contributing, thin filament activation is low even at high calcium concentrations. This would allow for SA to operate at high calcium concentrations.

For *Drosophila* and *Lethocerus* TnC1s to produce such significant functional differences, there must be differences in the structure of the TnCs, or in the interactions with other troponin components. The coordinating residues in the two active EF hands of the TnCs in the two species are identical (Qiu et al. 2003); however, the non-coordinating residues in the Ca^{2+}-binding loops differ, which may result in different calcium binding affinities. Sequence variation outside the calcium binding loops may also affect calcium affinity. The affinity of *Drosophila* TnC1 for calcium has not been measured, and the tertiary structure is not known, so it is not clear how much these factors contribute to the functional differences. The TnI and tropomyosin in *Drosophila* and *Lethocerus* IFM have different structures: *Lethocerus* TnI has a proline-alanine-rich C-terminal extension, and a similar sequence is fused to a tropomyosin isoform in *Drosophila*. Thus, it is likely that the troponin complexes in the two species would have different properties. The lattice structure of the *Drosophila* and *Lethocerus* IFMs are different (Squire et al. 2006), which may also contribute to the different mechanical properties.

Acknowledgments

References

Agianian B, Krzic U, Qiu F, Linke WA, Leonard K, Bullard B. A troponin switch that regulates muscle contraction by stretch instead of calcium. Embo J. 2004; 23:772–779. [PubMed: 14765112]

Bullard B, Pastore A. Regulating the contraction of insect flight muscle. J Muscle Res Cell Motil. 2011; 32:303–313.10.1007/s10974-011-9278-1 [PubMed: 22105701]

Burkart C, et al. Modular proteins from the Drosophila sallimus (sls) gene and their expression in muscles with different extensibility. J Mol Biol. 2007; 367:953–969. [PubMed: 17316686]

Card G, Dickinson M. Performance trade-offs in the flight initiation of Drosophila. J Exp Biol. 2008; 211:341–353. [PubMed: 18203989]

Collins JH. Myosin light chains and troponin C: structural and evolutionary relationships revealed by amino acid sequence comparisons. J Muscle Res Cell Motil. 1991; 12:3–25. [PubMed: 2050809]

Cullen MJ. The distribution of asynchronous muscle in insects with special reference to the Hemiptera: an electron microscope study. J Entomol. 1974; 49A:17–41.

Dickinson MH, et al. Phosphorylation-dependent power output of transgenic flies: an integrated study. Biophys J. 1997; 73:3122–3134. [PubMed: 9414224]

Esch H, Goller F, Heinrich B. How do bees shiver. Naturwissenschaften. 1991; 78:325–328.10.1007/Bf01221422

Farman GP, Miller MS, Reedy MC, Soto-Adames FN, Vigoreaux JO, Maughan DW, Irving TC. Phosphorylation and the N-terminal extension of the regulatory light chain help orient and align the myosin heads in Drosophila flight muscle. J Struct Biol. 2009; 168:240–249. [PubMed: 19635572]

Fukuda N, Granzier HL. Titin/connectin-based modulation of the Frank–Starling mechanism of the heart. J Muscle Res Cell Motil. 2005; 26:319–323.10.1007/s10974-005-9038-1 [PubMed: 16453158]

Gagne SM, Li MX, McKay RT, Sykes BD. The NMR angle on troponin C. Biochem Cell Biol. 1998; 76:302–312. [PubMed: 9923699]

Granzier HLM, Wang K. Interplay between passive tension and strong and weak binding cross-bridges in insect indirect flight muscle. J Gen Physiol. 1993; 101:235–270. [PubMed: 7681097]

Heinrich, B. The thermal warriors: strategies of insect survival. Harvard University Press; Cambridge: 1996.

Herranz R, Diaz-Castillo C, Nguyen TP, Lovato TL, Cripps RM, Marco R. Expression patterns of the whole troponin C gene repertoire during Drosophila development. Gene Expr Patterns. 2004; 4:183–190.10.1016/j.modgep.2003.09.008 [PubMed: 15161098]

Hyatt CJ, Maughan DW. Fourier analysis of wing beat signals: assessing the effects of genetic alterations of flight muscle structure in Diptera. Biophys J. 1994; 67:1149–1154. [PubMed: 7811927]

Iwamoto H, Inoue K, Yagi N. Fast X-ray recordings reveal dynamic action of contractile and regulatory proteins in stretch-activated insect flight muscle. Biophys J. 2010; 99:184–192. [PubMed: 20655846]

Josephson RK, Malamud JG, Stokes DR. Asynchronous muscle: a primer. J Exp Biol. 2000; 203:2713–2722. [PubMed: 10952872]

Josephson RK, Malamud JG, Stokes DR. The efficiency of an asynchronous flight muscle from a beetle. J Exp Biol. 2001; 204:4125–4139. [PubMed: 11809787]

Katzemich A, et al. The function of the M-line protein obscurin in controlling the symmetry of the sarcomere in the flight muscle of Drosophila. J Cell Sci. 2012; 125:3367–3379.10.1242/jcs.097345 [PubMed: 22467859]

Krzic U, Rybin V, Leonard KR, Linke WA, Bullard B. Regulation of oscillatory contraction in insect flight muscle by troponin. J Mol Biol. 2010; 397:110–118.10.1016/j.jmb.2010.01.039 [PubMed: 20100491]

Lakey A, Labeit S, Gautel M, Ferguson C, Barlow DP, Leonard K, Bullard B. Kettin, a large modular protein in the Z-disc of insect muscles. EMBO J. 1993; 12:2863–2871. [PubMed: 8335002]

Lehman W, Galinska-Rakoczy A, Hatch V, Tobacman LS, Craig R. Structural basis for the activation of muscle contraction by troponin and tropomyosin. J Mol Biol. 2009; 388:673–681.10.1016/j.jmb.2009.03.060 [PubMed: 19341744]

Lehmann FO, Dickinson MH. The changes in power requirements and muscle efficiency during elevated flight force production in the fruit fly. Drosophila J Exp Biol. 1997; 200:1133–1143.

Linari M, Reedy MK, Reedy MC, Lombardi V, Piazzesi G. Ca-activation and stretch-activation in insect flight muscle. Biophys J. 2004; 87:1101–1111. [PubMed: 15298914]

McKillop DF, Geeves MA. Regulation of the interaction between actin and myosin subfragment 1: evidence for three states of the thin filament. Biophys J. 1993; 65:693–701. [PubMed: 8218897]

Moss RL, Fitzsimons DP. Frank–Starling relationship: long on importance, short on mechanism. Circ Res. 2002; 90:11–13. [PubMed: 11786511]

Perz-Edwards RJ, et al. X-ray diffraction evidence for myosin-troponin connections and tropomyosin movement during stretch activation of insect flight muscle. Proc Natl Acad Sci USA. 2011; 108:120–125.10.1073/pnas.1014599107 [PubMed: 21148419]

Pringle JWS. Stretch activation of muscle: function and mechanism. Proc R Soc Lond B. 1978; 201:107–130. [PubMed: 27795]

Pringle JWS. The Bidder Lecture, 1980 the evolution of fibrillar muscle in insects. J Exp Biol. 1981; 94:1–45.

Qiu F, Lakey A, Agianian B, Hutchings A, Butcher GW, Labeit S, Bullard B. Troponin C in different insect muscle types: identification of an isoform in Lethocerus, Drosophila and Anopheles that is specific to asynchronous flight muscle in the adult insect. Biochem J. 2003; 371:811. [PubMed: 12558500]

Ramanath S, Wang Q, Bernstein SI, Swank DM. Disrupting the myosin converter-relay interface impairs Drosophila indirect flight muscle performance. Biophys J. 2011; 101:1114–1122.10.1016/j.bpj.2011.07.045 [PubMed: 21889448]

Reedy MC, Beall C. Ultrastructure of developing flight muscle in Drosophila. I Dev Biol. 1993; 160:443–465.

Reedy MC, Beall C, Fyrberg E. Formation of reverse rigor chevrons by myosin heads. Nature. 1989; 339:481–483.10.1038/339481a0 [PubMed: 2725681]

Rome LC, et al. Trading force for speed: why superfast crossbridge kinetics leads to superlow forces. Proc Natl Acad Sci USA. 1999; 96:5826–5831. [PubMed: 10318969]

Rosenfeld SS, Taylor EW. Kinetic studies of calcium binding to regulatory complexes from skeletal muscle. J Biol Chem. 1985; 260:252–261. [PubMed: 3965450]

Squire JM, et al. The myosin filament superlattice in the flight muscles of flies: a-band lattice optimisation for stretch-activation? J Mol Biol. 2006; 361:823–838.10.1016/j.jmb.2006.06.072 [PubMed: 16887144]

Swank DM. Mechanical analysis of Drosophila indirect flight and jump muscles. Methods. 2012; 56:69–77.10.1016/j.ymeth.2011.10.015 [PubMed: 22079350]

Swank DM, Knowles AF, Suggs JA, Sarsoza F, Lee A, Maughan DW, Bernstein SI. The myosin converter domain modulates muscle performance. Nat Cell Biol. 2002; 4:312–317. [PubMed: 11901423]

Swank DM, Kronert WA, Bernstein SI, Maughan DW. Alternative N-terminal regions of Drosophila myosin heavy chain tune muscle kinetics for optimal power output. Biophys J. 2004; 87:1805–1814. [PubMed: 15345559]

Syme DA, Josephson RK. Influence of muscle length on work from trabecular muscle of frog atrium and ventricle. J Exp Biol. 1995; 198:2221–2227.

Thorson J, White DCS. Role of cross-bridge distortion in the small-signal mechanical dynamics of insect and rabbit skeletal muscle. J Physiol (Great Britain). 1983; 343:59–84.

Tohtong R, Yamashita H, Graham M, Haeberle J, Simcox A, Maughan D. Impairment of muscle function caused by mutations of phosphorylation sites in myosin regulatory light chain. Nature. 1995; 374:650–653. [PubMed: 7715706]

Tu MS, Dickinson MH. The control of wing kinematics by two steering muscles of the blowfly (Calliphora vicina). J Comp Physiol. 1996; 178:813–830. [PubMed: 8667294]

Vibert P, Craig R, Lehman W. Steric-model for activation of muscle thin filaments. J Mol Biol. 1997; 266:8–14. [PubMed: 9054965]

Wang Q, Zhao C, Swank DM. Calcium and stretch activation modulate power generation in Drosophila flight muscle. Biophys J. 2011; 101:2207–2213.10.1016/j.bpj.2011.09.034 [PubMed: 22067160]

Wang Q, Newhard CS, Ramanath S, Sheppard D, Swank DM. An embryonic myosin converter domain influences Drosophila indirect flight muscle stretch activation, power generation and flight. J Exp Biol. 2014; 217:290–298.10.1242/jeb.091769 [PubMed: 24115062]

Wray JS. Filament geometry and the activation of insect flight muscles. Nature. 1979; 280:325–326.

Yang C, Ramanath S, Kronert WA, Bernstein SI, Maughan DW, Swank DM. Alternative versions of the myosin relay domain differentially respond to load to influence Drosophila muscle kinetics. Biophys J. 2008; 95:5228–5237. [PubMed: 18805920]

Zumstein N, Forman O, Nongthomba U, Sparrow JC, Elliott CJ. Distance and force production during jumping in wild-type and mutant Drosophila melanogaster. J Exp Biol. 2004; 207:3515–3522. [PubMed: 15339947]
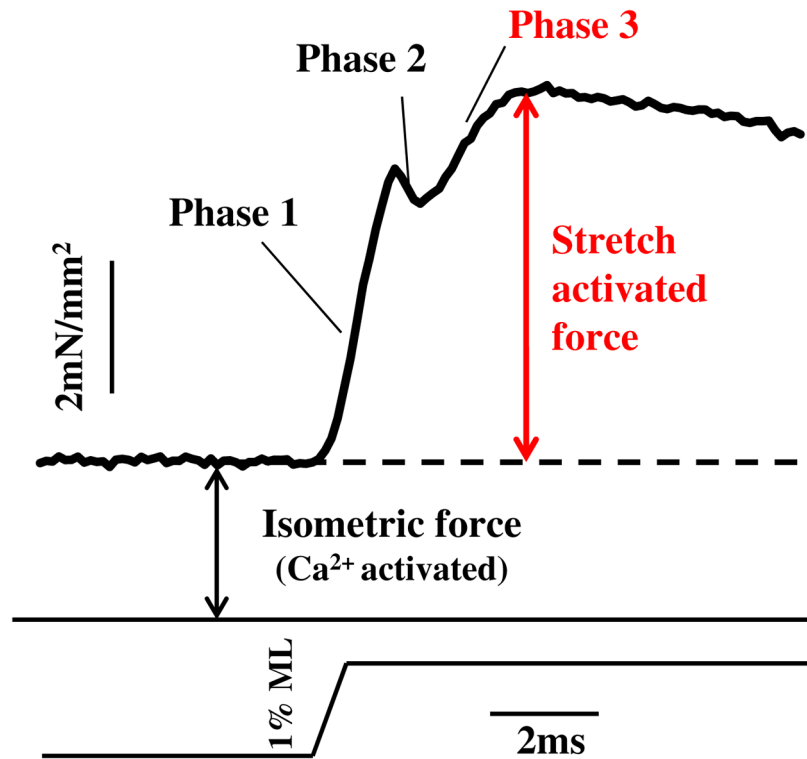
Fig. 1.
Stretch activation. Stretch activation is a delayed increase in force, phase 3, following a sudden increase in muscle length. Skinned IFM fiber at pCa 5.0
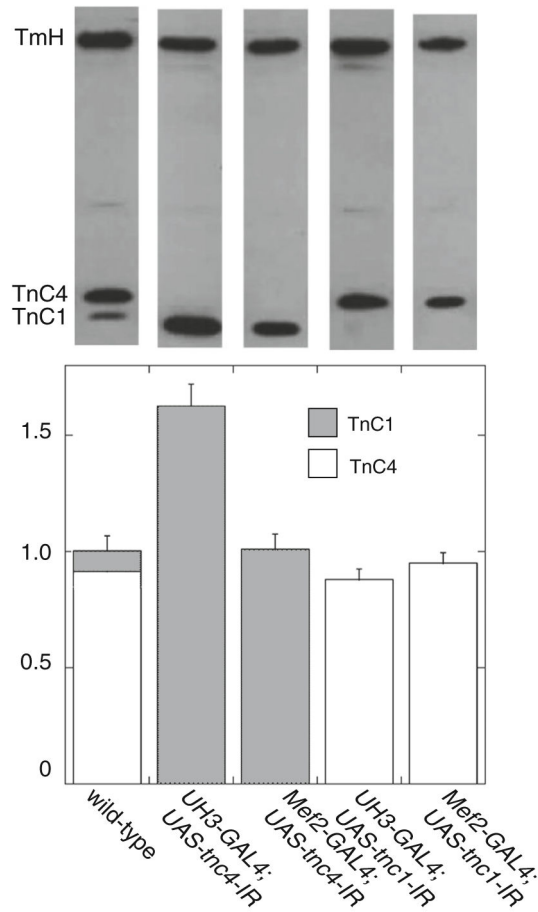
Fig. 2.
Levels of TnC4 and TnC1 in IFM. *Top* Blots of RNAi lines incubated with anti-TnC and anti-TmH (a loading control). *Bottom* Estimates of the amount of TnC4 and TnC1 in flies with reduced TnC. In IFM of wild type flies, the ratio of TnC4:TnC1 is about 10:1. In both *UH3-GAL4;UAS-tnc4-IR* and *Mef2-GAL4;UAS-tnc4-IR* flies, there is no detectable TnC4. Expression of TnC1 in these flies is increased using both drivers: with *UH3-GAL4*, the amount of TnC1 is 60 % greater than the total TnC in wild type flies, while in flies driven by *Mef2-GAL4*, TnC1 is increased to the level of total TnC in the wild type. In *UH3-GAL4;UAS-tnc1-IR* and *Mef2-GAL4;UAS-tcn1-IR* flies, there is no TnC1 and the amount of TnC4 is about the same as in the wild type. Values are calculated relative to amounts of TmH and normalized to the total TnC in IFM of wild type flies, $n = 4$ for all fly lines
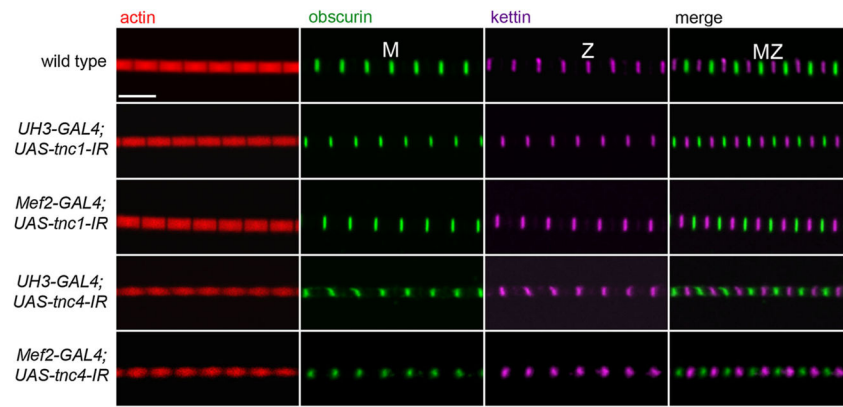
Fig. 3.

The effect of reduced TnC expression on the structure of the IFM. The regularity of the sarcomere was determined by labeling actin with phalloidin (*red*), the M-line with anti-obscurin (*green*) and the Z-disc with anti-kettin (*magenta*). Reduced TnC1 in the RNAi lines driven by *UH3-GAL4* or *Mef2-GAL4* had no discernible effect on the sarcomere structure. In TnC4 RNAi lines with both drivers, M-lines and Z-discs were dot-like and more diffuse than in the wild type. *Scale bar* 5 μm
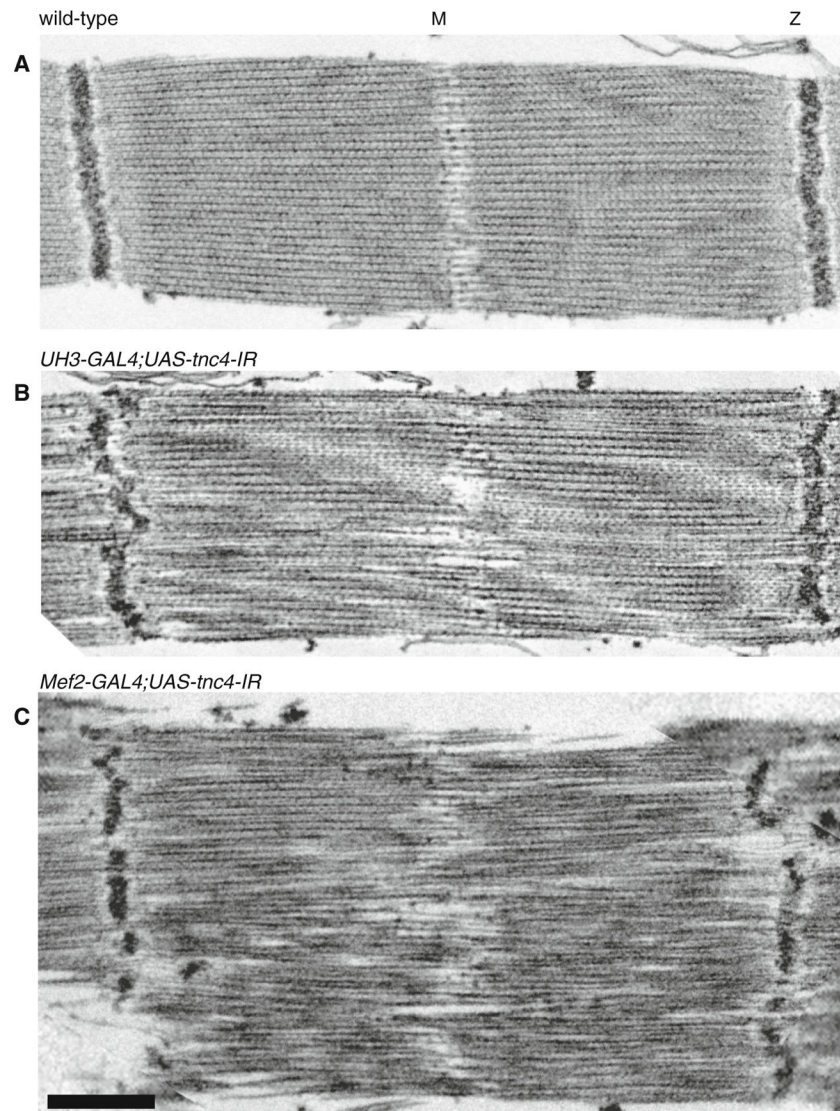
wild-type   M   Z

Fig. 4.
The structure of the IFM in flies with reduced TnC4. EM images of **a** wild type, **b** *UH3-GAL4;UAS-tnc4-IR* and **c** *Mef2-GAL4;UAS-tnc4* flies. The myofibrillar lattice is disrupted in knockdown flies driven with *UH3-GAL4* or *Mef2-GAL4*; Z-discs are irregular and there is no clear H-zone. The periphery of the sarcomere is ill defined in flies with the *Mef2-GAL4* driver. *Scale bar* 500 nm
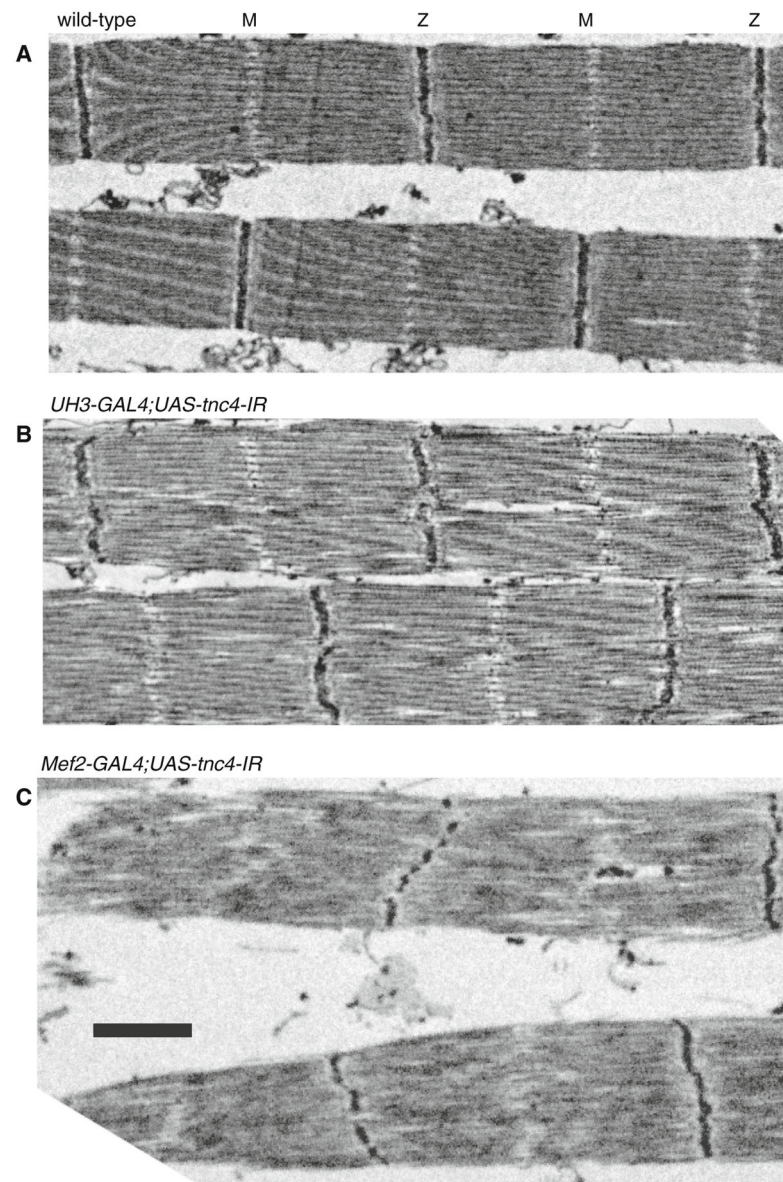
Fig. 5.
Overview of IFMs in flies with reduced TnC4. EM images of **a** wild type, **b** *UH3-GAL4;UAS-tnc4-IR* and c *Mef2-GAL4;UAS-tnc4-IR* flies. Sarcomere lengths of the knockdown flies are similar to those of the wild type; in flies with the *Mef2-GAL4* driver, the Z-disc is often broken up and sarcomeres are more irregular than in those with the *UH3-GAL4* driver. *Scale bar* 1 μm
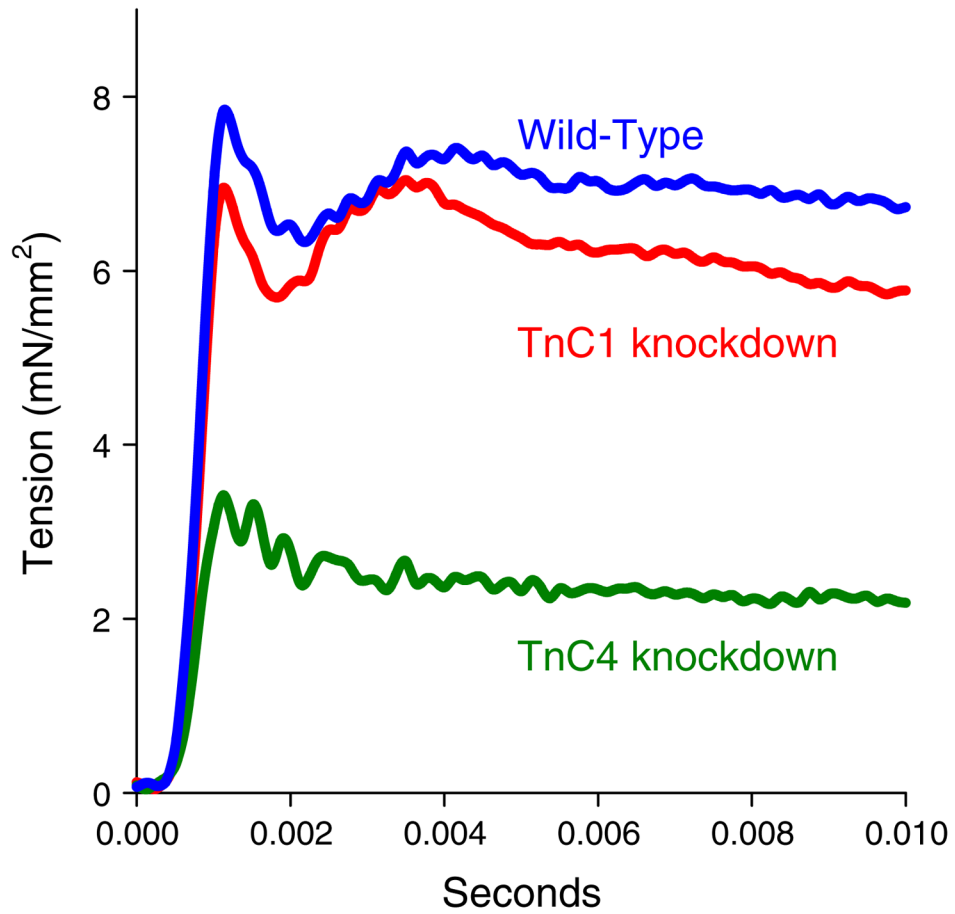
Fig. 6.
Representative tension traces from WT, TnC1-knockdown, and TnC4-knockdown IFM fibers in response to a 1 % ML stretch over 0.5 ms at pCa 5.0. Isometric tension immediately prior to stretch was subtracted so that starting tension is 0 for all traces
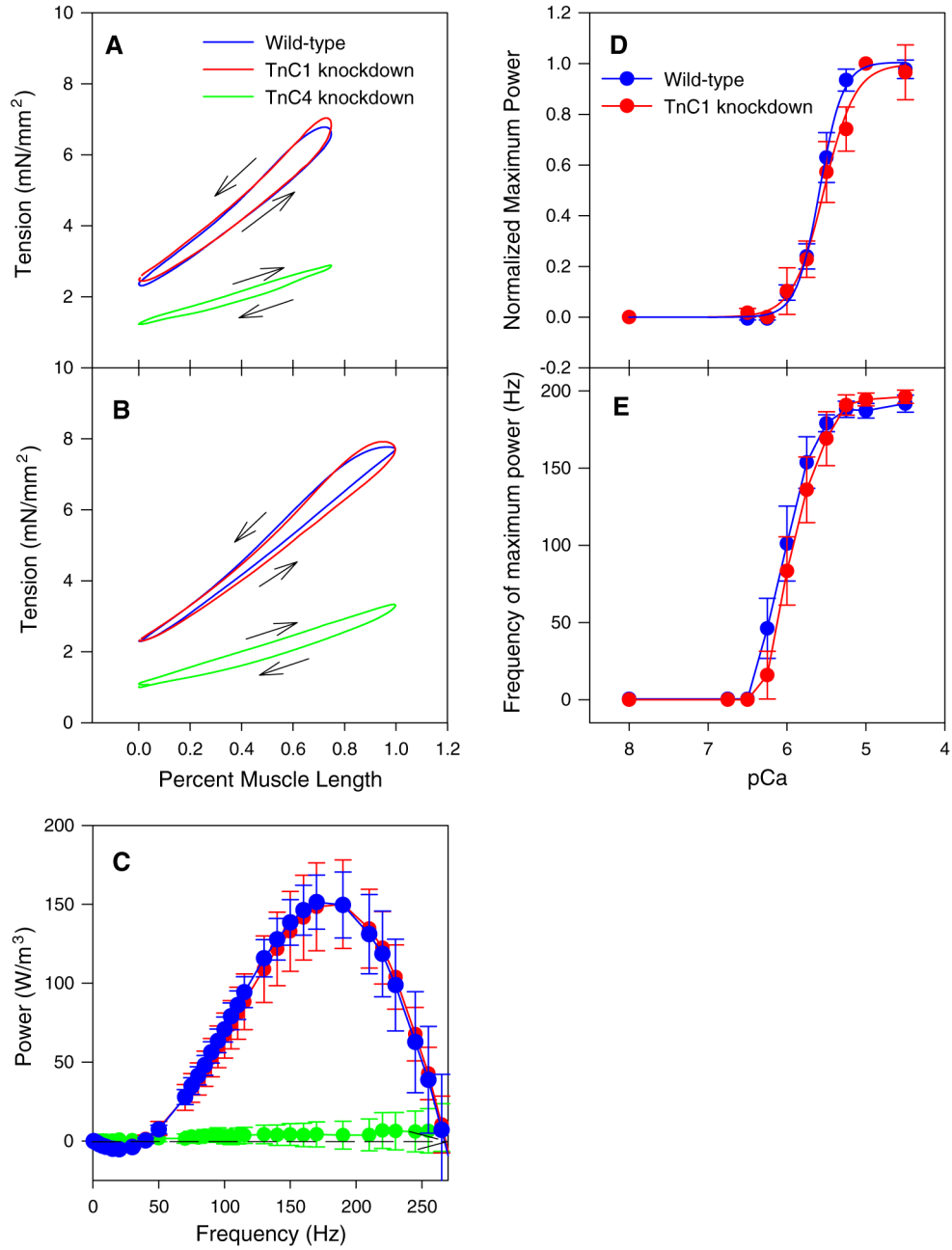
Fig. 7.
TnC4-knockdown eliminated positive work and power, but TnC1-knockdown had no effect on work or power. **a** Representative IFM work loops oscillated at a length change of 0.75 % ML and 100 Hz, pCa 5.0. *Arrows* indicate direction of work loops. Counterclockwise work loops indicate net positive work generating fibers and clockwise indicates work absorption. Both control and TnC1-knockdown fibers produced counter-clockwise work loops indicating they produce work and power while TnC4-knockdown fibers were clockwise indicating net work and power absorption. **b** Representative IFM work loops oscillated at a length change of 1 % ML amplitude, 125 Hz, pCa 5.0. **c** Power output by active (pCa 5.0)

IFM fibers plotted against small amplitude, 0.125 % ML, sinusoidal oscillation frequency. No differences in the amount of power at any frequency or the frequency at which maximal power output occurs (f_{max}) were observed between TnC1 knockdown and WT fibers. No power was produced by TnC4-knockdown fibers at any frequency. $N = 10$ for both lines. **d** Power-pCa curve for TnC1-knockdown and WT IFMs normalized to 1 at pCa 5.0. Mean ± S.E.M. $N = 12$ for WT and TnC1-knockdown, $N = 6$ for TnC4 knockdown. **e** The frequency at which maximum power was generated (f_{max}) was the same for TnC1-knockdown and WT IFMs at all calcium concentrations. Mean ± S.E.M. $N = 10$ for both lines
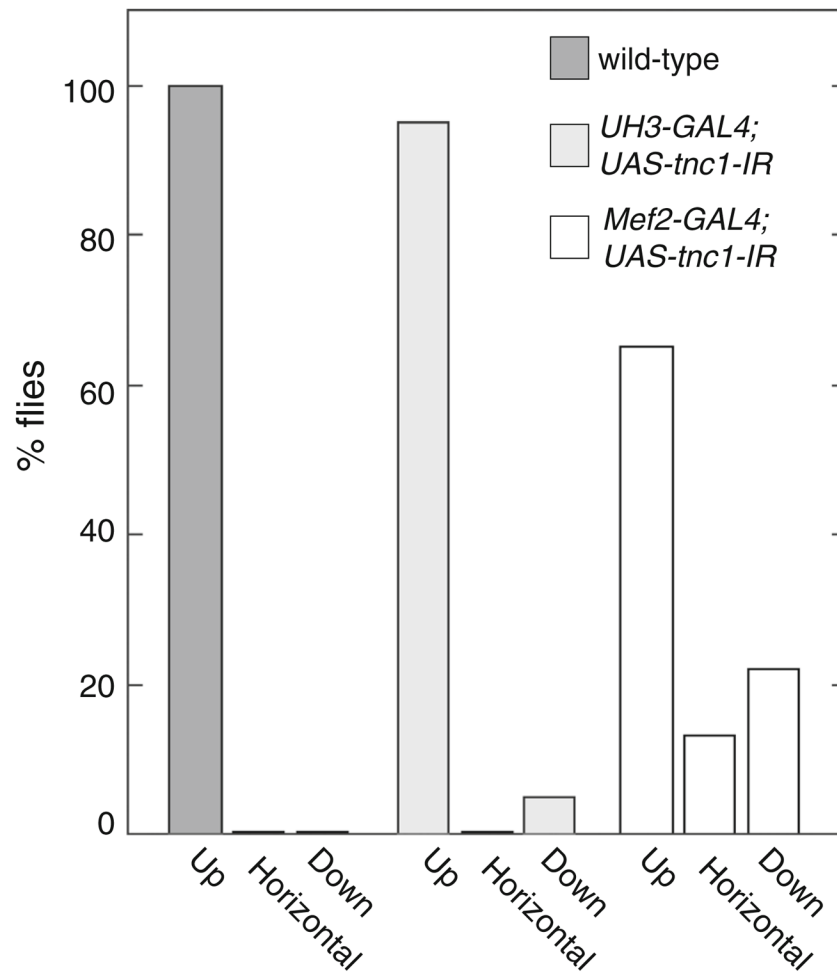
Fig. 8.
Flight ability of TnC1 knockdown flies is reduced, but only when using the *Mef2-GAL4* driver. Wild type flies and flies with knocked-down TnC were tested for upward and horizontal flight and no flight (down). All wild type and most of the *UH3-GAL4;UAS-tnc1-IR* flies flew upwards. Over 60 % of *Mef2-GAL4;UAS-tnc1-IR* flies flew upwards; some flew horizontally or not at all. *UH3-GAL4;UAS-tnc4-IR* and *Mef2-GAL4;UAS-tnc4- IR* flies were flightless (not shown). The flight ability of 20–30 flies was tested for each line

Table 1

Isometric tension of *Drosophila* indirect flight muscles

Fiber type	A_o (mN/mm^2)	P_o (mN/mm^2)	F_o (mN/mm^2)
TnC1 knockdown	4.5 ± 0.4 ($n = 27$)	2.7 ± 0.4 ($n = 27$)	1.8 ± 0.2 ($n = 27$)
TnC4 knockdown	$1.4 \pm 0.2^*$ (n = 5)	$1.0 \pm 0.2^*$ ($n = 5$)	$0.4 \pm 0.2^*$ ($n = 5$)
Wild-Type	4.1 ± 0.4 ($n = 23$)	2.5 ± 0.2 ($n = 23$)	1.6 ± 0.2 ($n = 23$)

Values are mean ± S.E.M. Both knockdown lines were generated by crossing with the *Mef2-Gal4* driver line

n number of fibers; A_0 total isometric tension measured at pCa 5.0, 15 °C, P_0 passive tension measured at pCa 8.0, F_0 net active isometric tension after subtracting passive tension ($F_0 = A_0 – P_0$)

$^*P < 0.05$, significantly different from wild-type (*Mef2-Gal4* line) as determined by Student's *t* test, 2-tailed, type 2

Table 2

Stretch-activated tension in IFM

Fiber type	A_{SA} (mN/mm²)	P_{SA} (mN/mm²)	F_{SA} (mN/mm²)
TnC1 knockdown ($n = 11$)	5.3 ± 0.5	3.9 ± 0.5	1.4 ± 0.2
Wild-type ($n = 10$)	4.8 ± 0.5	3.5 ± 0.4	1.5 ± 0.2

All values are mean ± S.E.M. Length step was 1 % of muscle length, 0.5 ms duration. Tension was measured at the peak of the phase 3 response. TnC4 knockdown fibers did not produce a phase 3 response (SA). Both knockdown lines were generated by crossing with the *Mef2-Gal4* driver line

n number of fibers; A_{SA} total active stretch tension at pCa 5.0; P_{SA} passive stretch tension at pCa 8.0; F_{SA} corrected active stretch tension ($F_{SA} = A_{SA} - P_{SA}$)

Table 3

Work and power generation by *Drosophila* IFM

Fiber type	Work (nJ/mm^3)	Power (W/m^3)
TnC1 knockdown (*n* = 11)	2.2 ± 0.3	217 ± 33
TnC4 (*n* = 5) knockdown	−1.5 ± 0.1[*]	−149 ± 14[*]
Wild-type (*n* = 9)	1.3 ± 0.4	130 ± 43

Values are mean ± S.E.M. Measurements were made at 0.75 % ML Amp, 100 Hz, pCa5 using the work loop technique. Both knockdown lines were generated by crossing with the *Mef2-Gal4* driver line

n number of fibers

[*]*P* < 0.05, significantly different from both WT (*Mef2-Gal4* line) and TnC1 knockdown fibers as determined by Student's *t* test

Table 4

Sinusoidal analysis of IFM fibers

Fiber type	Maximum power (W/m³)	Frequency of maximum power (Hz)	Frequency of maximum work (Hz)	pCa$_{50}$	Hill coefficient
TnC1 knockdown	179.5 ± 2.3 (n = 14)	190.0 ± 4.3 (n = 14)	155.4 ± 4.2 (n = 13)	5.5 ± 0.09 (n = 10)	4.1 ± 0.6 (n = 10)
Wild-type	176.5 ± 6.0 (n = 12)	195.8 ± 5.7 (n = 12)	155.8 ± 6.2 (n = 12)	5.6 ± 0.04 (n = 10)	4.8 ± 0.6 (n = 10)

No data are presented for TnC4 knockdown fibers because no positive power was generated by TnC4 knockdown fibers. Values are mean ± S.E.M

n number of fibers

Table 5

Wing beat frequency

Fly line	21 °C WBF, (Hz)	15 °C WBF (Hz)
UH3-Gal4;UAS-tnc1-IR	205.8 ± 1.6 ($n = 23$)	163.6 ± 1.7 ($n = 23$)
UH3-Gal4 (control)	202.7 ± 1.9 ($n = 23$)	160.6 ± 1.4 ($n = 23$)
Mef2-Gal4;UAS-tnc1-IR	202.0 ± 2.0 ($n = 23$)	160.3 ± 1.9[*] ($n = 21$)
Mef2-Gal4 (control)	201.2 ± 3.1 ($n = 19$)	169.6 ± 2.9 ($n = 19$)

Assays were performed at 21 and 15 °C

[*] $P < 0.05$ significantly different from control, Student's *t* test